Biosensors and Bioelectronics 25 (2010) 2464–2469

Contents lists available at ScienceDirect

Biosensors and Bioelectronics

journal homepage: www.elsevier.com/locate/bios

Simultaneous determination of biomarkers for Alzheimer's disease using sol–gel-derived optical array biosensor

Ruey-an Doong*, Pin-Shang Lee, Kowthalam Anitha

101, Sec. 2, Kuang Fu Road, Department of Biomedical Engineering and Environmental Sciences, National Tsing Hua University, Hsinchu 30013, Taiwan

ARTICLE INFO

Article history:
Received 8 December 2009
Received in revised form 2 April 2010
Accepted 6 April 2010
Available online 14 April 2010

Keywords:
Array-based biosensor
Sol–gel
Alzheimer's disease (AD)
Fluorescent dye
β-Amyloid
Multianalytes

ABSTRACT

The sol–gel-derived optical array-based biosensor for the simultaneous analysis of multiple analytes as potential markers for Alzheimer's disease was fabricated. β-Amyloid, acetylcholine and glutamate were selected as the biosensing probes. The fluorescent dye, carboxy SNARF-1-dextran, was co-immobilized with glutamate dehydrogenase and acetylcholinesterase for sensing glutamate and acetylcholine, respectively, while Amplex red and FITC-dextran were immobilized with horseradish peroxidase for determination of β-amyloid and hydrogen peroxide (H_2O_2). The biosensors exhibited a good performance on simultaneous analysis of multianalytes without obvious cross-interference and the detection limits of H_2O_2, β-amyloid, glutamate and acetylcholine were 1.57 nM, 0.63 nM, 0.55 μM, and 1.0 μM, respectively. The developed array biosensors were also applied to determine multianalytes in human serum samples spiked with various concentrations of analytes and showed a good analytical performance with dynamic range of 4 orders of magnitude for β-amyloid. Results obtained in this study clearly demonstrate the possibility of using a sol–gel-derived optical array-based biosensor for simultaneous analysis of multiple samples in the presence of important analytes for Alzheimer's disease.

1. Introduction

Alzheimer's disease (AD) is a progressive neurodegenerative disorder affecting a large proportion of the aging population. AD is characterized by gradual loss of cognitive function and synaptic integrity, selective neuronal death and abnormal formation of neurotic and core plaques in the cerebral cortex (Schoonenboom et al., 2004; Blennow et al., 2006). The interest in using amyloid and other neurotransmitters as laboratory markers to confirm the diagnosis of AD arises from the evidence that cerebral accumulation of the β-amyloid peptide growth formed by aggregation in diseased tissue (Cannon et al., 2004). AD is also a synaptic disease that involves the concentration change in various neurotransmitter systems, particularly those where synaptic transmission is mediated by acetylcholine (Ach) or glutamate (Glu). Furthermore, β-amyloid peptide, the most proteinaceous component of the extracellular amyloid deposits produced from proteolytic protein, is believed to be one of the key substances underlying the pathogenesis of AD because of its strong ability to complex with metal ions (Cu^{2+}, Zn^{2+}, Fe^{2+}) (Brzyska et al., 2001; Schoonenboom et al., 2004). In addition, the aggregation of β-amyloid can induce the accumulation of hydrogen peroxide (H_2O_2) and overproduction of reactive oxygen species and free radicals in neurons (Bush, 2003).

Several methods including commercial ELISA kit (Levy et al., 2007), mass spectroscopy (Portelius et al., 2006) and localized surface plasma resonance (LSPR) spectroscopy (Perez et al., 2004; Hirohata et al., 2007) can provide the rapid and correct determination of amounts of β-amyloid in body fluids of the AD patients. Several studies have developed the electrochemical biosensing systems aiming at the specific measurement of acetylcholine for investigating therapeutics of AD (Lenigk et al., 2000; Du et al., 2007). More recently, the optical biosensors based on LSPR or surface enhanced Raman spectroscopy (SERS) for detection of β-amyloid have been developed (Rahmam et al., 2005; Wilson and Gifford, 2005; Favero et al., 2005; Chou et al., 2008; Vestergaard et al., 2008). Although the concentration level of each metabolite in biofluids has its unique clinical meaning, simultaneous determination of these important chemicals can provide more information as potential markers of AD. It is therefore of importance to develop array-based biosensor system for simultaneous determination of AD-related analytes.

The potential of using array-based biosensors for diverse purposes such as antibody screening, monitoring of enzyme reactions, environmental pollutants, protein–protein interactions, and diagnostics have been explored (Doong et al., 2005; Tehan et al., 2007; Borisov and Wolfbeis, 2008). Fluorescent-based optical transduction is one of the promising tools for fabrication of array-based biosensors because it provides good sensitivity and specificity

* Corresponding author. Tel.: +886 3 5726785; fax: +886 3 5718649.
E-mail address: radoong@mx.nthu.edu.tw (R.-a. Doong).

0956-5663/$ – see front matter © 2010 Elsevier B.V. All rights reserved.
doi:10.1016/j.bios.2010.04.005

as well as decreased background noise in biomedical analysis (Cho et al., 2002; Grant et al., 2005; Wolfbeis, 2005; Ramanathan and Simonian, 2007). The immobilization method is important in fabrication of array-based biosensor because it governs the stability and applicability of the developing system. A previous study has demonstrated that the addition of polyvinyl alcohol (PVA) can retain at least 30% activity of enzymes in silica sol–gel materials (Tsai and Doong, 2007), demonstrating that the sol–gel method is one of the promising techniques which can encapsulate biomolecules in porous materials to preserve the catalytic activity of enzymes under suitable conditions.

In this study, an enzymatically fluorescent array-based biosensor for the determination of AD-related multianalytes was developed. Several analytes including β-amyloid, H_2O_2, Glu, and ACh, which are considered as potential indicators of AD, were selected. The effect of metal ions including Cu^{2+}, Mn^{2+} and Zn^{2+} on the determination of β-amyloid was also investigated. In addition, human serum samples spiked with different analytes were used to evaluate the potential application of the array-based biosensor to real samples.

Two different principles based on the ratiometric measurement of pH change were designed for determination of multianalytes as well as for minimization of possible interferences derived from the deviations of spot sizes. For ACh and Glu determination, a proton is produced after the hydrolysis of ACh and Glu by their corresponding enzymes, acetylcholinesterase (AChE) and glutamate dehydrogenase (Gldh) (Eqs. (1) and (2)). Therefore, the pH-sensitive fluorescent dye, carboxy SNARF-1-dextran, was used as the indicator for measurement. When carboxy SNARF-1-dextran was excited at 520 nm, the acid tautomer of carboxy SNARF-1-dextran emitted with a peak in the 580–590 nm range, while the emission peak of the base form appeared in the range 630–640 nm (Gulcev et al., 2002). Therefore, the intensity ratio of acid and base forms (I_{640}/I_{580}) was used for ratiometric measurement of multianalytes and minimization of variation of spot sizes.

$$(CH_3)_3\overset{\oplus}{N}CH_2CH_3O\overset{O}{\overset{\|}{C}}CH_3 \xrightarrow{AChE} (CH_3)_3\overset{\oplus}{N}CH_2CH_3OH + CH_3COOH \quad (1)$$

$$l\text{-glutamate} + H_2O + NADP^+ \overset{GLDH}{\rightleftharpoons} 2\text{-Oxoglutarate} + NH_3 + NADPH + H^+ \quad (2)$$

The FITC co-immobilized with Amplex red were used as the sensitive dyes for determination of β-amyloid and H_2O_2 in the presence of HRP (Eq. (3)). Since β-amyloid can complex with metal ions and result in the formation of H_2O_2, Cu^{2+} ion was used in this study to enhance the analytical performance of array-based biosensors via production of H_2O_2. The hydrogen peroxide was subsequently consumed by HRP to produce a strong fluorescence at 590 nm as a result of the reduction of Amplex red to resorufin. It is noted that the spot sizes in sol–gel elements varied slightly (<15%) during the pin-printing process (Cho et al., 2002). Therefore, another pH-sensitive fluorescent dye, FITC-dextran, was co-encapsulated in the sol–gel to minimize possible interferences of spot sizes (Tsai and Doong, 2004). The fluorescence intensity ratio of Amplex red/FITC-dextran (AF ratio) was then used to enhance the sensitivity of the determination of β-amyloid sensing system.

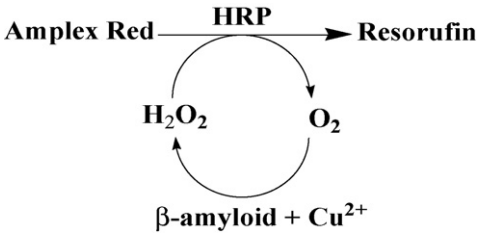

(3)

2. Experimental

2.1. Reagents

Acetylcholinesterase (AChE, EC 3.1.1.7) from electric eel (type VI-S349 units/mg-solid), glutamate dehydrogenase (Gldh, EC 1.4.1.4) from *Proteus* species (447 units/mg-protein), horseradish peroxidase (HRP, EC 1.11.1.7) from horseradish (type X, 13 mg-protein/mL), acetylcholine chloride (monosodium salt, 99%), L-glutamic acid (monosodium salt, 99%), β-nicotinamide adenine dinulcleotide phosphate hydrate (NADP), 3-bis [tris (hydroxymethyl) methylamino] propane (BTP buffer, 99%) and fluorescein isothiocyanate-dextran (FITC-dextran) were obtained from Sigma chemicals (St. Louis, MO). Polyvinyl acetate (PVAc) and polyvinyl alcohol (PVA) were purchased from Aldrich (Milwaukee, WI) and Fluka Chemicals (Buchs, Switzerland), respectively. Tetramethyl orthosilicate (TMOS, 98%) was obtained from Tokyo Chemical Inc. (Tokyo, Japan). Amplex red and carboxy SNARF-1-dextran were purchased from Molecular Probes (Eugene, Oregon). All other chemicals were of analytical grade and were used as received without further purification. A 50-well chambered coverslip (ϕ 3 mm × 1 mm, spacing 4.5 mm) was obtained from Grace Bio-Labs Inc. (Bend, OR).

Enzyme solutions including AChE (250 U/mL) and Gldh (250 U/mL) were prepared in 5 mM BTP buffer at pH 6.8, while HRP (250 U/mL) was prepared at pH 8.0. The fluorescent dye, SNARF-1-dextran (5.0 mg/mL), FITC-dextran (1000 μg/mL), and Amplex red (5 mM) were also prepared in 5 mM BTP buffer at pHs 7, 7.5, and 8.5, respectively. All aqueous were prepared by bidistilled deionized water (bdH_2O) (18.3 MΩ cm) unless otherwise mentioned. The room temperature was controlled at 19 ± 1 °C and the relative humidity was in the range 55–75%. The $K_2Cr_2O_7/H_2SO_4$ clean solution was prepared by dissolving 0.84 g of $K_2Cr_2O_7$ in 7 mL of H_2O and then 200 mL of concentrated H_2SO_4 was added slowly.

2.2. Sol–gel preparation

The sol–gel method, which has been proven to be an effective method of the immobilization of biomolecules, was used to prepare the array-based biosensor according to the procedures described in our previous studies (Tsai and Doong, 2004, 2005, 2007; Doong and Shih, 2006, 2010). The sol stock solution was prepared by adding 555 μL of TMOS and 135 μL of 1 mM HCl in a glass vial. The mixture was sonicated for 30 min at 20 °C to complete the acid-catalyzed reaction and to obtain a clear and homogeneous solution. The sol solution was stored at 4 °C and was used within 2 weeks.

2.3. Preparation of array-based biosensor

Glass microscope slides (2.5 cm × 7.5 cm) were cleaned with $K_2Cr_2O_7/H_2SO_4$ solution for 2 h to remove trace organic contaminants. After washing with copious amounts of bidistilled H_2O and drying under a gentle stream of N_2 gas, the glass slides were dipped into PVAc solution (5% in dichloromethane) for 1 h to enhance the sol–gel attachment. The slides were then removed from the container slowly, purged with N_2, and stored under ambient con-

ditions until used. A 50-well chambered coverslip was affixed on the PVAc-coated slide, and placed on a thermoelectric cooler stage for contact printing (Tsai and Doong, 2005). The sol–gel-derived array-based biosensor was printed automatically using a three-dimensional robotic system controlled by a LabVIEW program. The 50 sol–gel spots (5 × 10), each with an individual well, were printed within 5 min. The volume used for the sol–gel spot, controlled by the robotic system, was 200 nL and the spot size was about 800 μm. Subsequently, the array was gelled for 20 min under ambient conditions. Ten microliters of BTP buffer was then loaded into the wells to stabilize the sol–gel for 1 h prior to being used for analysis.

2.4. Analytical procedure and fluorescence detection

The multiple samples in the presence of multianalytes were simultaneously analyzed using the sol–gel-derived array biosensor. 15 μL of sample solutions containing BTP buffer (blank control), β-amyloid, ACh, and/or Glu were added into the array-based biosensor. For Ach and Glu determination, the sol–gel mixture was obtained by mixing 5 μL of SNARF-dextran, 5 μL of glycerol, 7 μL of PVA (4% in H_2O), 10 μL of sol stock solution and 10 μL of enzyme solution. For preparation of β-amyloid biosensors, the sol–gel mixture was obtained by mixing 5 μL of Amplex red (5 mM) and FITC-dextran (1000 μg/mL) solution, 10 μL of enzyme solution, 5 μL of glycerol, 7 μL of PVA (4%) and 10 μL stock sol solution. The concentrations were in the range 0.01–10 μg/mL for β-amyloid and 0.01 − 10 mM for ACh and Glu. In addition, effects of pH values, Cu^{2+}, and incubation time on the determination of β-amyloid at 25 °C were examined. The values used for optimization were 6.0–7.0 for pH, 5 μM to 5 mM for Cu^{2+}, and 5–20 min for incubation time. After the incubation at desired time, solutions were removed and the ratiometric fluorescence intensities were measured (Tsai and Doong, 2005; Doong and Shih, 2006).

The cross-reactivity in the presence of multianalytes for β-amyloid determination were examined by adding 0.01–100 μM Ach or Glu into the solutions containing 0.5 mM Cu-complexed β-amyloid and fluorescent dyes. In addition, the metal solutions of Zn^{2+} and Mn^{2+} in the concentration range 0.01–100 μM were added into the biosensing system to investigate the competitive effect of metal ion with Cu^{2+}. The applicability of the optical biosensors to biological sample was also evaluated by spiking various concentrations of β-amyloid (0.01–100 μg/mL), Ach (5–10000 μM) and Glu (5–10000 μM) into human serums after 5 times dilution using BTP buffer.

Fig. S1 (see Supplementary Information) shows the schematic illustration of the developed system for the fluorescence detection (Doong and Shih, 2010). The fluorescence microscope equipped with an objective lens (10×, numerical aperture 0.3) and a blue-enhanced silicon detector with a 100 mm^2 sensing area (Edmund Industrial Optic Inc., Barrington, NJ) was used for fluorescence detection. Two filter blocks, G-2A (excitation (EX) 510–560 nm, dichroic mirror (DM) 575 nm, barrier filter (BA) 590 nm, Nikon) and B-2A (EX 450–490 nm, DM 505 nm, BA 520 nm, Nikon) were used for the detection of the emission spectra of fluorescent dyes including SNARF-1-dextran, Amplex red and FITC-dextran. An optical chopper with a 5/6 slot blade (SR540, Stanford Research System, Sunnyvale, CA) was set at the frequency of 392 Hz to minimize the electronic interference. The signal obtained from the silicon detector was integrated with the chopper reference by a signal-board lock-in amplifier (FEMTO Messtechnik GmbH, Berlin, Germany). The data was acquired by the data acquisition card (DAQ card, PCI-1200, National Instruments, TX). The fluorescence intensity of each spot was measured automatically by scanning over the sol–gel spots by the developed robotic and optical systems programmed by the LabVIEW™ software (National Instruments, TX).

3. Results and discussion

3.1. pH effect on sol–gel-derived biosensors

The microenvironments of the sol–gel-derived biosensors in terms of elemental ratio, surface morphology, specific surface area, and pore size were investigated to characterize the physicochemical properties of PVA-modified sol–gel materials (Tsai and Doong, 2007). Results showed that the sol–gel-derived method is an effective method for preservation of enzyme activity. In addition, the sol–gel preparation conditions such as gelation time, porosity, morphology, and enzyme activity can influence the performance of the array-based biosensors (Tsai and Doong, 2004, 2005). The pH value was found to be one of the most important factors controlling the analytical performance of the biosensor. Therefore, the effect of pH value on the fluorescence intensity as well as analytical performance was first examined.

In this study, the emission of carboxy SNARF-1 in BTP buffer solution showed that the fluorescence fell predominantly in a band centered at 580 nm at pH 6–7, while a new emission peak centered near 640 nm was observed when pH values increased to higher than 8 (Supplementary Information, Fig. S2). In addition, the fluorescence intensity ratio (I_{640}/I_{580}) of the dye molecule in the sol–gel-derived film increased with the increase in pH values (Supplementary Information, Fig. S3), which is in good agreement with the previous results (Doong and Shih, 2010; Gulcev et al., 2002). This increase in fluorescent intensity in sol–gel matrix may be attributed to the increase in the apparent pK_a (7.8) of SNARF-1-dextran and the effective increase in concentration of fluorescent probe during the drying process. The isoelectric point (pI) of SiO_2 is 2.0–4.0, which means that the positively charged SNARF-1-dextran would be associated with the negatively charged SiO_2 surface. During the gelation process, the association of SNARF dye and SiO_2 surface may improve the fluorescence quantum efficiency in sol–gel-derived matrix due to the increase in the apparent concentration in sol–gel film. Therefore, the intensity ratio of I_{640}/I_{580} is a suitable indicator used to determine the concentrations of ACh and Glu.

Fig. S4 (see Supplementary Information) shows the pH response profile of the sol–gel-derived biosensor array. The AF ratio increased with increasing pH value and reached a plateau when the pH was higher than 8.5. The relative standard deviation (RSD) was found to be in the range 0.6–4.9%, depicting that the dual-fluorescence calibration can significantly minimize the interference. In addition, the pK_a value, determined from the inflection point of the curve, was 6.2 ± 0.1, which is in good agreement with the thermodynamic protolytic constant of fluorescein in solution (pK_a = 6.4) and the FITC-dextran entrapped in PVA-based biofilm (pK_a = 6.2 ± 0.1) (Liu et al., 2000). These results clearly demonstrate that both SNARF-1-dexrean and AF ratio are capable of detecting pH values precisely and can be used for determination of multianalytes in sol–gel-derived array biosensors.

3.2. Determination of β-amyloid and H_2O_2

The effects of solution pH, Cu^{2+} concentration, and incubation time on β-amyloid determination were first optimized. Fig. 1 shows the effects of Cu^{2+} concentration and pH value on the biosensor performance toward β-amyloid determination. The Cu^{2+} concentration and pH of Cu^{2+} solution are substantial parameters dominating the sensitivity and dynamic range of the optical array biosensor. In the presence of 5 mM Cu^{2+}, the dynamic range of β-amyloid was only 2 orders of magnitude (1–100 μg/mL) at pH 6.0, presumably due to the fact that the production of H_2O_2 is too fast to react with Amplex red and HRP. In contrast, a dynamic range of 3 orders of magnitude (0.1–100 μg/mL) for β-amyloid was

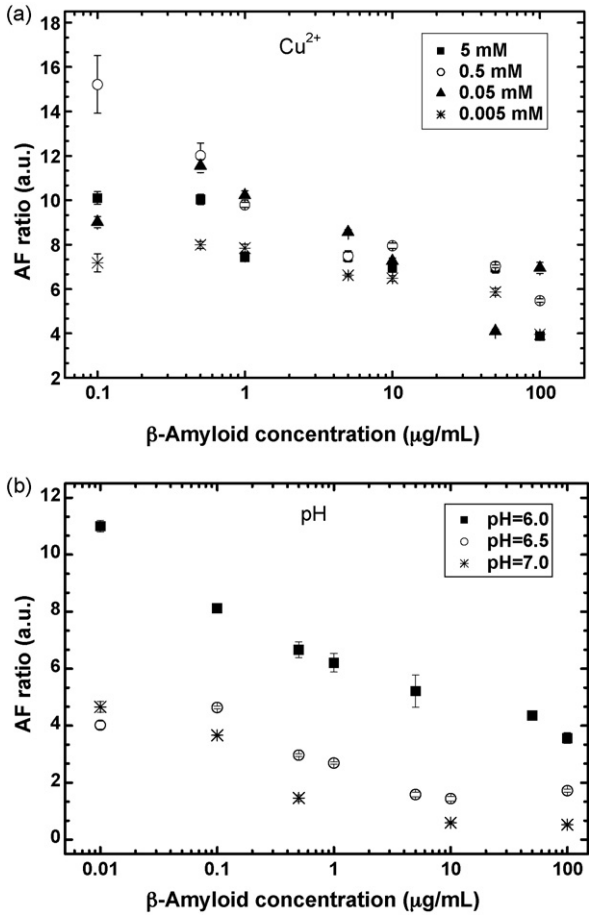

Fig. 1. Effects of (a) Cu^{2+} concentration and (b) pH value on the determination of β-amyloid using the horseradish peroxidase-encapsulated array biosensors. The AF ratio represents the ratio of fluorescence intensity between Amplex red and FITC-dextran.

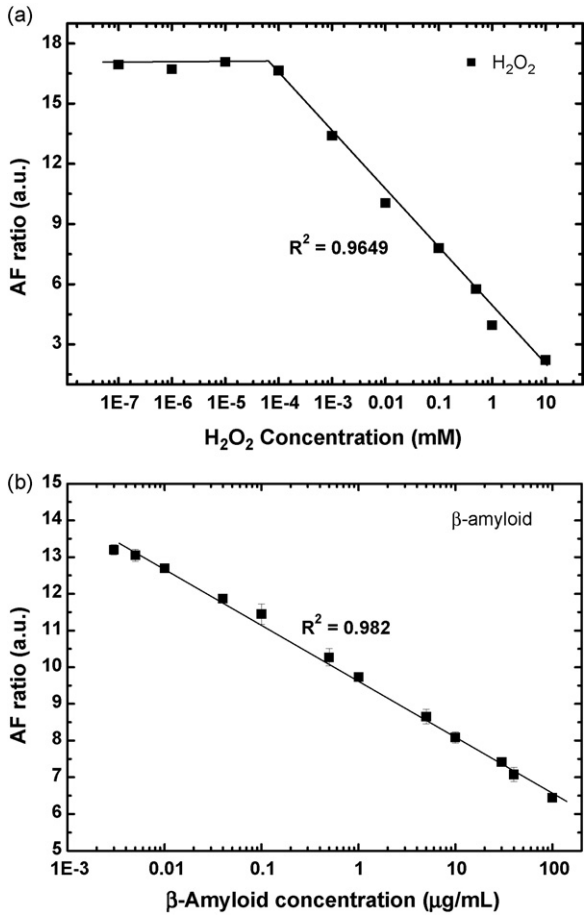

Fig. 2. Response of the array-based biosensor toward the determination of (a) β-amyloid and (b) hydrogen peroxide.

achieved when 0.5 mM Cu^{2+} were used. The linear range decreased to 1–100 μg/mL again when further decreased the Cu^{2+} concentration to 5–50 μM at pH 6.0, clearly showing that addition of 0.5 mM Cu^{2+} is the optimal concentration for the biosensor to exhibit better analytical performance.

The pH effect of Cu^{2+} solutions was examined in the range 6.0–7.0 to understand the performance of the sensor system and to minimize the precipitation of copper hydroxide ($Cu(OH)_2$). As shown in Fig. 1b, the linear range of the sensor system was <3 orders of magnitude at pH 6.5–7.0. On the contrary, a linear range of 0.01–100 μg/mL, which corresponds to 4 orders of magnitude at pH 6.0 was obtained. This means that the production of H_2O_2 by complexation of Cu^{2+} with β-amyloid at low pH is better than that at high pH. In addition, different incubation times were also optimized. Fig. S5 (see Supplementary Information) shows the AF ratio as a function of incubation time ranging from 5 min to 60 min at 25 °C. The AF ratio increased upon increasing incubation time from 5 min to 20 min and then reached the plateau. Further increase in incubation time did not enhance the analytical performance of the array-base biosensor. Therefore, an incubation time of 20 min was chosen for further experiments.

To evaluate the biosensor performance, the fluorescent intensity was measured with the introduction of various concentrations of β-amyloid to the sampling wells. The experiments were carried out after incubation of 20 min under the optimized conditions at pH 6.0 in the presence of 0.5 mM Cu^{2+}. Fig. 2 shows the response curves of array-based biosensors toward β-amyloid and H_2O_2. The linear range of β-amyloid was 4 orders of magnitude (0.01–100 μg/mL) with r^2 of 0.982. In addition, the RSD and limit of detection (LOD) were 8.5% and 2.5 ng/mL, respectively. Several studies have used gold nanoparticle-based optical methods including SERS and LSPR to detect β-amyloid using nanofludic or immuno-biosensors. Vestergaard et al. (2008) fabricated a gold-capped nanoparticle LSPR-based immunochip for detection of τ protein, and found that the LOD of τ protein could be lower to 10 pg/mL after the incubation of 1 h. However, no linear range was reported. A previous study has developed a specific and reliable competitive affinity assay kit for measurement of neural thread protein and found that the dynamic range was in the range 10–60 μg/mL (Levy et al., 2007). Although the detection limit obtained in this study is higher than the reported data by immunochip, the response time of the developed method is short (20 min). In addition, the developed biosensor has a wide dynamic range for β-amyloid determination and is the first enzymatic biosensor for determination of β-amyloid and related analytes fluorescently, which has the advantages of easy fabrication, low cost and rapid response.

Hydrogen peroxide is one of the reactive oxygen metabolic byproducts serving as a key regulator for a number of oxidative stress-related sites. The developed array biosensor can also be applied to determine H_2O_2 individually. As depicted in Fig. 2b. The fluorescent intensity decreased upon increasing H_2O_2 concentrations, and a linear range of 0.1–10,000 μM with the LOD of 1.57 nM was observed. This result clearly demonstrates that the oxidation of Amplex red is linked to HRP-catalyzed oxidation of Cu-complexed β-amyloid by oxygen under the experimental conditions.

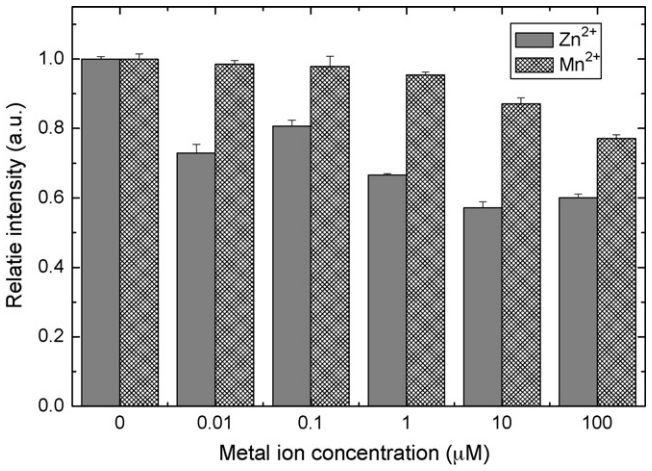

Fig. 3. Effect of metal ions on the determination of β-amyloid by array-based biosensors. The metal ions used in this study were Zn^{2+} and Mn^{2+} at concentration range of 0.01–100 μM.

3.3. Determination of acetylcholine and glutamate

In order to prepare a pH-based array biosensor for ACh and Glu determination, different initial pH values and buffer concentrations were optimized to evaluate the sensor performance. The biosensor showed good sensitivity when 5 mM BTP buffer at pH 9.0 was used. When ACh and Glu were catalyzed by their corresponding enzymes, protons were produced to lower the pH value of system. Therefore, the response of biosensors at high pH value showed a better sensitivity than that at low ones. Both the linear ranges of Ach and Glu were 3 orders of magnitude and the RSDs were 2.5% and 5% ($n = 5$), respectively. In addition, the LODs for ACh and Glu were 1.02 μM and 0.53 μM, respectively, which are 50 and 10 times lower than the previous studies on AChE-encapsulated array co-immobilized with a pH-sensitive dye FITC-dextran (50 μM) (Tsai and Doong, 2005) and GLdh-encapsulated titania sol–gel optical biosensor array (5.5 μM) (Doong and Shih, 2006).

3.4. Simultaneous determination of multianalytes

One of the major advantages of the array-based biosensor is the capability of simultaneous detection of multiple samples in the presence of multiple analytes. Since each sol–gel spot has its own reaction chamber in the array biosensor, the determination of multianalytes under different conditions can be performed by simply adding different microsamples into the reaction chambers. To understand the potential of the simultaneous determination of multiple samples and cross-reactivity in the presence of multianalytes for β-amyloid determination, various concentrations of different substrates including Ach and Glu ranging from 0.01 μM to 100 μM were spiked into the solutions containing Cu-complexed β-amyloid and fluorescent dyes. In addition, two metal solutions (Zn^{2+} and Mn^{2+}) at 0.01–100 μM, serving as the competitive substrates with Cu^{2+}, were added into the biosensing system. No obvious inhibition effect of other neurotransmitters on the determination of β-amyloid was observed. This means that neither Glu nor Ach will affect the determination of β-amyloid using the array-based biosensor. However, addition of metal ions competed β-amyloid with copper ion, resulting in the decrease in sensitivity of array-based biosensor. Fig. 3 shows the effects of metal ions on the β-amyloid determination. Addition of Mn^{2+} at concentrations lower than 10 μM had little effect on β-amyloid determination. However, a 20–30% decrease in signal intensity was observed when Mn^{2+} concentrations increased to 10–100 μM. In contrast, Zn^{2+} had strong ability to complex with β-amyloid, and subsequently decreased the signal intensity of the sensing system. Addition of 0.01–1 μM Zn^{2+} decreased the signal intensity to its original 70–80%, and then to 57–60% when further increased the concentration to 10–100 μM. It is noted that Mn^{2+} concentration in biofluids is usually low, while serum Zn^{2+} concentrations generally fall within the range 12–17 μM in healthy adults (Arnaud et al., 2008). This indicates that the presence of Zn^{2+} in biofluids may have a higher interference effect on β-amyloid determination than that of Mn^{2+}.

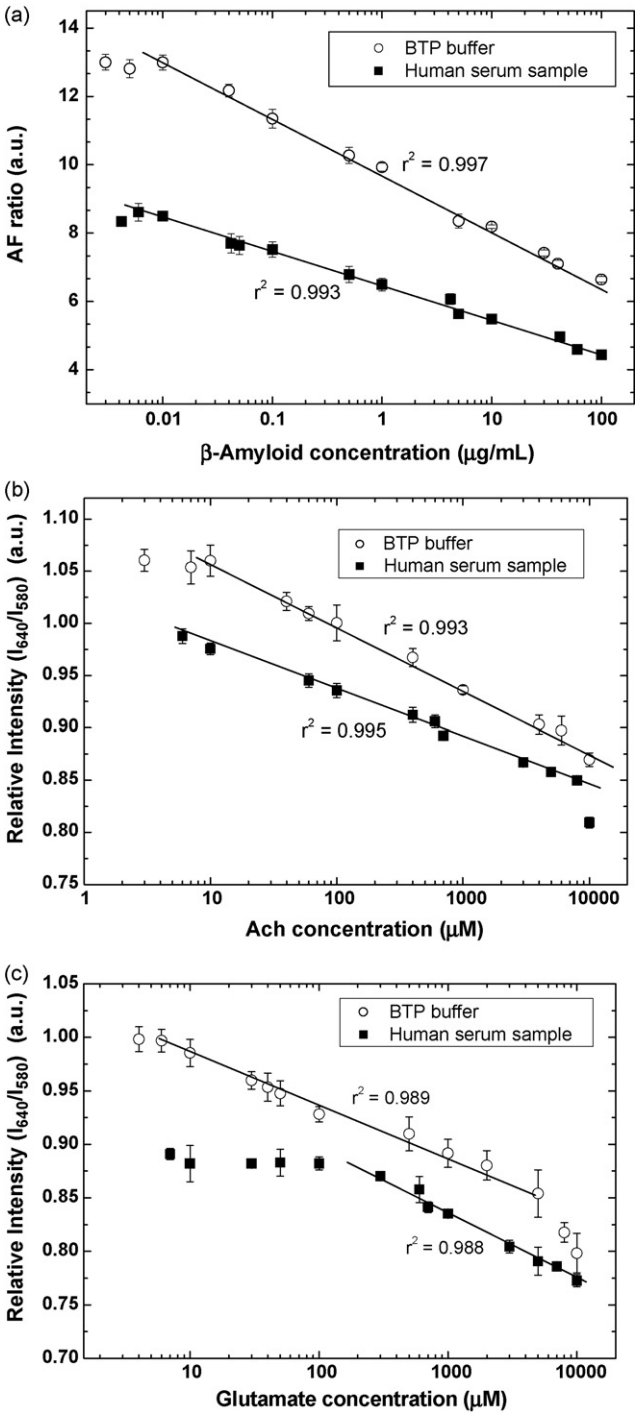

Fig. 4. Response of the array biosensor toward the determination of (a) β-amyloid, (b) acetylcholine, and (c) glutamate in buffer solutions and human serum samples.

Since the detection principle of Glu and ACh is based on the change in pH value, the cross-reactivity of ACh and Glu was further examined by spiking various concentrations of neurotransmitters into BTP buffer. Fig. S6 (see Supplementary Information) shows the cross-reactivity of neurotransmitter on the determination of ACh and Glu. No obvious inhibition or synergistic effects on the determination of ACh concentration was observed when Glu concentrations were in the range 10–1000 μM. In contrast, the existence of ACh caused cross-reactivity in the Glu sensor system because of the quick hydrolysis of ACh in solution, resulting in the decrease in pH value of the biosensing system. This means that the existence of ACh causes a negative effect on Glu determination, especially at high concentrations of ACh.

3.5. Application to spiked samples

The applicability of the optical biosensors to biological sample analysis was evaluated by spiking various concentrations of β-amyloid, ACh and Glu into human serums after 5 times dilution using BTP buffer. Fig. 4 illustrates the responses of the array-based biosensor toward various concentrations of anlaytes in human serum samples. The linear range of β-amyloid in real samples was in the range 0.01–100 μg/mL, which corresponds to 4 orders of magnitude with r^2 of 0.993. In addition, the LODs of β-amyloid in real sample and buffer solution were 2.3 ng/mL and 2.5 ng/mL, respectively. However, the slopes of linearity for real sample and BTP buffer were 1.63 and 0.95, respectively, depicting that there may exist matrix effects on the determination of β-amyloid in real human serum samples.

The response of AChE-encapsulated array biosensors toward ACh in human serum was also investigated (Fig. 4b). The linear range of Ach in this sensor system for real sample reached about 3 orders of magnitude with r^2 of 0.995 (5–9000 μM). The response curve of Ach in buffer solution also showed the linear range of 3 orders of magnitude. However, the LODs of ACh were observed to be 1.02 μM for real sample and 0.30 μM for buffer solution. Similar result was also observed for Glu determination. As depicted in Fig. 4c, the analytical range of Glu by Gldh-encapsulated array biosensors in real samples was in the range 100–10,000 μM with r^2 of 0.988. The linear ranges of Glu in real samples and buffer solutions were 2 and 3 orders of magnitude with LODs of 4.5 μM and 0.53 μM, respectively. These results clearly show that the sol–gel-derived array-based biosensors exhibit their ability to the determination of β-amyloid and related metabolites in spiked human serum samples.

4. Conclusions

In this study, the silica sol–gel-derived array-based optical biosensor which can simultaneously determine the potential biomarkers of AD including β-amyloid, ACh, and Glu along with H_2O_2 and pH was developed. We have demonstrated a simple method to rapidly immobilize enzymes and fluorescent dyes into the matrix. The developed biosensor array exhibits good analytical figures of merit with wide dynamic range of 4–5 orders of magnitude and low LODs, which provides a promising tool for screening the disease characteristics of these potential analytes. In addition, the biosensor arrays were successfully applied to biological analysis of multianalytes in spiked human serum samples. Also, the developed biosensors can determine hydrogen peroxide and pH effectively. Results obtained in this study clearly demonstrate the feasibility of fabrication of sol–gel-derived array-based optical biosensors with excellent performance for determination of β-amyloid, ACh and Glu in Alzheimer's disease.

Acknowledgement

The authors thank National Science Council (NSC), Taiwan for financial support under contract No. NSC 96-2113-M-007-027-MY3.

Appendix A. Supplementary data

Supplementary data associated with this article can be found, in the online version, at doi:10.1016/j.bios.2010.04.005.

References

Arnaud, J., Weber, J.-P., Weykamp, C.W., Parsons, P.J., Angerer, J., Mairiaux, E., Mazarrasa, O., Valkonen, S., Menditto, A., Patriarca, M., Taylor, A., 2008. Clin. Chem. 54 (11), 1892–1899.
Blennow, K., de Leon, M.J., Zetterberg, H., 2006. Lancet 368 (9533), 387–403.
Borisov, S.M., Wolfbeis, O.S., 2008. Chem. Rev. 108 (2), 423–461.
Brzyska, M., Bacia, A., Elbaumi, D., 2001. Eur. J. Biochem. 268 (12), 3443–3454.
Bush, A.I., 2003. Trends in Neurosci. 26 (4), 207–214.
Cannon, M.J., Williams, A.D., Wetzel, R., Myszka, D.G., 2004. Anal. Biochem. 328 (1), 67–75.
Cho, E.J., Tao, Z., Tehan, E.C., Bright, F.V., 2002. Anal. Chem. 74 (24), 6177–6184.
Chou, I.H., Benford, M., Beier, H.T., Coté, G.L., Wang, M., Jing, N., Kameoka, J., Good, T.A., 2008. Nano Lett. 8 (6), 1729–1735.
Doong, R.A., Shih, H.M., Lee, S.H., 2005. Sens. Actuators B 111, 323–330.
Doong, R.A., Shih, H.M., 2006. Biosens. Bioelectron. 22 (2), 185–191.
Doong, R.A., Shih, H.M., 2010. Biosens. Bioelectron. 25 (6), 1439–1446.
Du, D., Chen, S.Z., Cai, J., Song, D.D., 2007. J. Electroanal. Chem. 611 (3), 60–66.
Favero, G., Campanella, L., Cavallo, S., D'Annibale, A., Perrella, M., Mattei, E., Ferri, T., 2005. J. Am. Chem. Soc. 127 (22), 8103–8111.
Grant, S.A., Pierce, M.E., Lichlyter, D.J., Grant, D.A., 2005. Anal. Bioanal. Chem. 381 (5), 1012–1018.
Gulcev, M.D., Goring, G.L.G., Rakic, M., Brennan, J.D., 2002. Anal. Chim. Acta 457 (1), 47–59.
Hirohata, M., Hasegawa, K., Tsutsumi-Yasuhara, S., Ohhashi, Y., Ookoshi, T., Ono, K., Yamada, M., Naiki, H., 2007. Biochemistry 46 (7), 1888–1899.
Lenigk, R., Lam, E., Lai, A., Wang, H., Han, Y., Carlier, P., Renneberg, R., 2000. Biosens. Bioelectron. 15 (9–11), 541–547.
Levy, S., McConville, M., Lazaro, G.A., Averback, P., 2007. J. Clin. Lab. Anal. 21 (1), 24–33.
Liu, Y.H., Dam, T.H., Pantano, P., 2000. Anal. Chim. Acta 419 (2), 215–225.
Perez, M., Cuadros, R., Benitez, M.J., Jimenez, J.S., 2004. J. Alzheimer's Dis. 6 (5), 461–467.
Portelius, E., Zetterberg, H., Andreasson, U., Brinkmalm, G., Andreasen, N., Wallin, A., Westman-Brinkmalm, A., Blennow, K., 2006. Neurosci. Lett. 409 (3), 215–219.
Rahmam, M.A., Kwon, N.H., Won, M.S., Choe, E.S., Shim, Y.B., 2005. Anal. Chem. 77 (15), 4854–4860.
Ramanathan, M., Simonian, A.L., 2007. Biosens. Bioelectron. 22 (12), 3001–3007.
Schoonenboom, N.S.M., Pijnenburg, Y.A.L., Mulder, C., Rosso, S.M., Van Elk, E.J., Van Kamp, G.J., Van Sweiten, J.C., Scheltens, P., 2004. Neurology 62 (9), 1580–1584.
Tehan, E.C., Higbee, D.J., Wood, T.D., Bright, F.V., 2007. Anal. Chem. 79 (14), 5429–5434.
Tsai, H.C., Doong, R.A., 2004. Anal. Biochem. 334 (1), 183–192.
Tsai, H.C., Doong, R.A., 2005. Biosens. Bioelectron. 20 (9), 1796–1804.
Tsai, H.C., Doong, R.A., 2007. Biosens. Bioelectron. 23 (1), 66–73.
Vestergaard, M., Kerman, K., Kim, D.K., Hiep, H.M., Tamiya, E., 2008. Talanta 74 (4), 1038–1042.
Wilson, G.S., Gifford, R., 2005. Biosens. Bioelectron. 20 (12), 2388–2403.
Wolfbeis, O.S., 2005. J. Mater. Chem. 15 (27–28), 2657–2669.